Extremely Narrow Plasmon Resonances Based on Diffraction Coupling of Localized Plasmons in Arrays of Metallic Nanoparticles

V. G. Kravets, F. Schedin, and A. N. Grigorenko

School of Physics and Astronomy, University of Manchester, Manchester, M13 9PL, United Kingdom

(Received 17 February 2008; published 22 August 2008)

We experimentally demonstrate extremely narrow plasmon resonances with half-width of just several nanometers in regular arrays of metallic nanoparticles. These resonances are observed at Rayleigh's cutoff wavelengths for Wood anomalies and based on diffraction coupling of localized plasmons. We show experimentally that reflection from an array of nanoparticles can be completely suppressed at certain wavelengths. As a result, our metal nanostructures exhibit π-jump for the phase of the reflected light.

DOI: 10.1103/PhysRevLett.101.087403 PACS numbers: 78.67.Bf, 71.45.Gm, 73.20.Mf

Plasmonic nanostructures have recently attracted a lot of attention with demonstration of extraordinary optical transmission [1–3], perfect lensing [4–6], magnetic response at visible wavelengths [7] and a promise of new optical elements [8,9]. A wide application of metallic nanoparticles and produced from them composite ''nanomolecules'', however, hindered by the fact that localized plasmon resonances (LPRs) are broad. It was argued that poor quality of LPR is a general property of an individual metallic nanoparticle [10]. While broad plasmon resonances may be beneficial to some applications, e.g., field amplifications [11], many other applications, such as nanolasers, nanolenses, negative index metamaterials [7], biosensing, etc., would get a strong boost from plasmon resonances of a higher quality factor Q.

A promising way to improve quality of LPRs is to utilize radiative field coupling in regular arrays of nanoparticles. Recently, Schatz *et al.* suggested that extremely narrow plasmon resonances are possible in regular arrays of nanoparticles [12]. The theory of narrow plasmon resonances has been elaborated by Markel [13]. Despite some experimental success in controlling the shape of plasmon resonances by radiative coupling [14], supernarrow plasmon resonances have not been observed. Here we report an experimental observation of extremely narrow resonances measured in sample absorption and reflection and produced by diffraction coupling of localized plasmons (LPs), similar in nature to Schatz-Markel resonances.

The underlying physics of the proposed resonances is simple. It is known that regular periodic structures can show abrupt changes in reflection, which are referred to as Wood anomalies [15]. For regular arrays of nanoparticles on a transparent substrate these anomalies have been explained by Rayleigh as a disappearance of a diffracted beam when it crosses the boundary between ambient medium (which we suppose to be air for simplicity) and substrate. A transition of a diffraction mode between air and substrate is not allowed due to different dispersion relations for light in both media. As a result, the diffraction mode is cut off at a so-called Rayleigh cutoff wavelength [16]. There are two types of Rayleigh cutoff wavelengths (λ_R)—one for the disappearance of an ''air'' diffraction mode (where a diffraction mode crosses the sample boundary from air to substrate) and another for the disappearance of a ''substrate'' diffraction mode (where a diffraction mode crosses the boundary from substrate to air) [16]. The air λ_R for a square array of a lattice constant a are given by

$$\lambda^{\mathrm{air}}_{R\_mpq} = \frac{a}{m}[\sqrt{p^2 + q^2} \pm \sin(\theta)\{p\cos(\varphi) + q\sin(\varphi)]\}$$

where m, p, and q are integers, θ is the angle of incidence (AOI) and φ is the polar angle of the substrate orientation with respect to the plane of incidence. For $\varphi = 0$ the most important air and substrate λ_R are given by

$$\lambda^{\mathrm{air}}_{R\_m} = \frac{a}{m}[1 \pm \sin(\theta)] \quad \text{and} \quad \lambda^{\mathrm{sub}}_{R\_m} = \frac{a}{m}[n_s \pm \sin(\theta)], \tag{1}$$

where m is an integer and n_s is the substrate refractive index. When an array is illuminated by a light of the Rayleigh cutoff wavelength, one of the diffracted waves travels exactly along the surface of the substrate (at a grazing angle) and hence interacts with many nanoparticles. Therefore, if λ_R is close to the wavelength of LPR for an individual nanoparticle one might hope to achieve strong transfer of energy from the incident beam into LP modes in a narrow wavelength range near a Wood anomaly and hence obtain sharp plasmon resonances. In this case the nanoparticles array would generate a mixed mode of LP vibrations combined with the diffracted grazing wave which will be resonantly excited by incident light.

To study this idea, we have used arrays of Au nanodots (nanopillars) fabricated by electron-beam lithography on a glass substrate. The structures covered an area of 200 μm $\times$ 200 μm and contained $\approx 10^6$ pillars. To perform electron-beam lithography, a 5 nm layer of Cr has been evaporated onto a glass substrate. The lattice constant, a, for the periodic square arrays was down to 270 nm. Heights h of Au pillars (3 nm Cr followed by 90 nm of Au) and their average diameters $d \approx 100$ nm were chosen so that LPR for nanopillars appeared at red-light wavelengths.

The dimensions are close to those demanded by Schatz-Markel theory [12,13].

Figure 1(a) shows typical extremely narrow resonances experimentally observed in reflection near $\lambda \approx 600$ nm at angles of incidence (AOI) of 62–68° for the square array of single Au nanoparticles with $a = 320$ nm (by a resonance in this Letter we imply a narrow feature in sample reflection/extinction produced by an excitation of a specific mode of electromagnetic field). The optical measurements have been performed with a Woollam ellipsometer which has a focusing spot down to 30 μm. The resonance is plotted in Ψ-Δ values routinely used in ellipsometry so that $E_p/E_s = \tan(\Psi)\exp(i\Delta)$, where E_p and E_s are the reflected field amplitudes for the incident light E_i of p and s polarizations, respectively, [17]. Figure 1(b) plots behavior of the relative phase Δ at the same AOIs and Fig. 1(c) provides the spectral dependence of the reflection coefficient $R_p = |E_p/E_i|$ and $R_s = |E_s/E_i|$. The deep and extremely narrow minimum with half-width of just 5 nm is observed in reflection of light of p polarization at $\lambda^{\text{air}}_{R\_1} = a(1 + \sin(\theta))$ of the air, and therefore can be identified with a Wood anomaly for the studied regular array of metallic nanodots [see also Figs. 3(d)–3(f) where λ_R are superimposed on the reflection spectra]. The inset of Fig. 1 (a) shows a zoom of Ψ near the resonance peak for AOI = 64° and the inset of Fig. 1(b) provides an analogous zoom for the phase Δ. From here we see that the reflection R_p goes close to zero while the phase Δ demonstrates dramatic changes for Wood anomaly at AOI = 64°, which is analogous to the behavior of light reflection from a dielectric material near the Brewster angle [18].

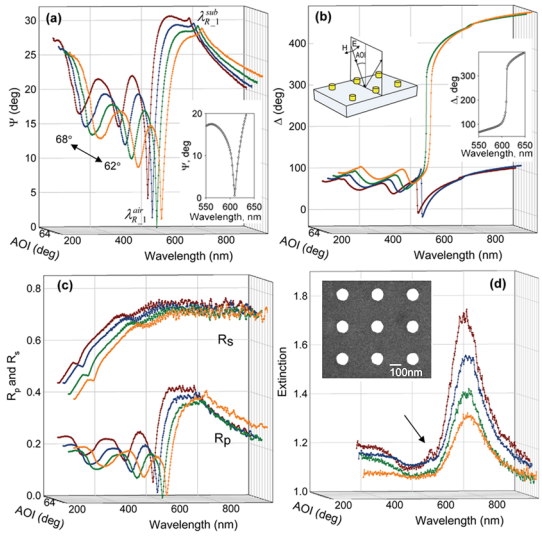

FIG. 1 (color online). Wood anomalies for the single dot Au nanoarray with the period $a = 320$ nm, the dot diameter $d = 100$ nm, the dot height $h = 90$ nm. Spectral dependences observed at AOI = 62° (orange curves), 64° (green), 66° (blue), 68° (brown) for (a) Ψ-value. The inset shows a zoom of the reflection dip at AOI = 64°. $\lambda^{\text{air}}_{R\_1}$ and $\lambda^{\text{sub}}_{R\_1}$ are given by (1) with the sign "+." (b) Phase Δ. The inset on the left shows the experimental geometry for the incident light of p polarization. The inset on the right shows a zoom of the phase jump at AOI = 64°. (c) Reflection R_p and R_s for light of p and s polarizations, respectively. (d) Extinction for p polarization. The inset shows the electron micrograph of the array. The arrow indicates the position of the weak narrow resonance in absorption.

Wood anomalies observed in reflection [Figs. 1(a)–1(c)] from the array of nanodots do not necessarily guarantee a sharp peak in extinction (and hence an excitation of LPR of nanoparticles). Indeed, measured extinction (the ratio of the incident light intensity over the transmitted intensity) for the same single particles array showed only a weak feature at the wavelength $\lambda = 600$ nm and only at large AOIs; see Fig. 1(d) where an arrow indicates a weak narrow peak at AOI = 68°. This is due to the fact that the Rayleigh cutoff wavelength for the studied singe dot array was far from the position of LPR of nanoparticles observed at about 700 nm; see Fig. 1(d). There are several ways to match LPR with λ_R for Wood anomaly: (i) to increase the array period, (ii) to decrease particle sizes or (iii) to change geometry of the unit cell of the array. In this work we have chosen the latter method.

To match λ_R with LPR, we have utilized double-dot geometry shown in the inset of the Fig. 2(d). At small

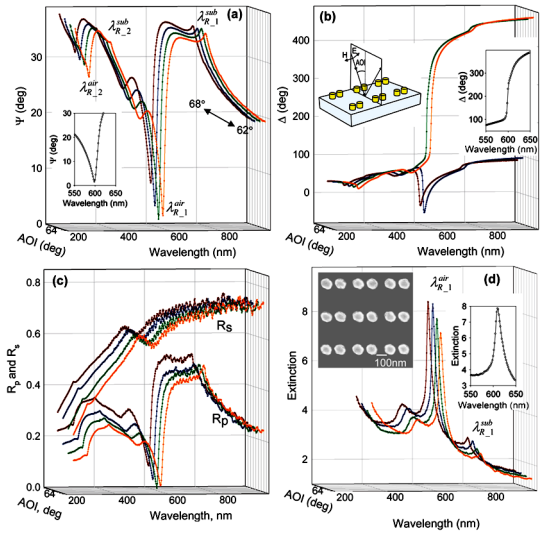

FIG. 2 (color online). Wood anomalies and supernarrow resonances for the double-dot Au nanoarray with the period $a = 320$ nm, the dot diameter $d = 108$ nm, the dot height $h = 90$ nm. AOI = 62° (orange curves), 64° (green), 66° (blue), 68° (brown) for (a) Ψ-value. The inset shows a zoom of the reflection dip at AOI = 64°. $\lambda^{\text{air}}_{R\_m}$ and $\lambda^{\text{sub}}_{R\_m}$ are given by (1) with the sign "+." (b) Phase Δ. The inset on the left shows the experimental geometry for the incident light of p polarization. The inset on the right shows a zoom of the phase jump at AOI = 64°. (c) Reflection R_p and R_s for light of p and s polarizations, respectively. (d) Extinction for p polarization. The electric field of the incident wave is perpendicular to the line connecting neighboring dots. The left inset shows the electron micrograph of the array. The right inset shows a zoom of a peak in extinction at AOI = 64°.

dot separations, electromagnetic interaction between neighboring dots within a pair splits LPR observed for an individual dot into two resonances for a dot pair [19–21]. The main resonance mode is redshifted for incident waves with electric field directed along the line connecting the neighboring dots and blueshifted for the waves with the electric field directed perpendicular to this line due to the dipole interaction [7,22]. As a result, the electromagnetic interaction shifts LPR from 700 nm for a nanodot ($d \approx$ 100 nm) to about 600 nm for the double-dot nanomolecules with the center-to- center separation in the pair $s =$ 140 nm.

Figure 2(a) shows extremely narrow resonances experimentally observed near $\lambda \approx 600$ nm at AOIs of 62–68° for the square array of double Au dots with the same period $a = 320$ nm, $d = 108$ nm, $s = 140$ nm. We see that the pronounced narrow resonance for the double-dot array is again observed in the phase of the reflected light, Fig. 2(b) and the reflection amplitudes, Fig. 2(c). In contrast to single dots, Wood anomaly of the double dots is coupled with the LPR of metallic nanomolecules and extinction also shows a remarkable narrow peak at almost $\lambda^{\text{air}}_{R\_1} = a(1 + \sin(\theta))$, see Fig. 2(d), Fig. 3(a), and especially Fig. 3 (b), which shows the spectral dependence of the absorption peak superimposed with the dependence of $\lambda^{\text{air}}_{R\_1}$ and $\lambda^{\text{sub}}_{R\_1}$. Figures 1 and 2 demonstrate the main result of this Letter—extremely narrow resonances for regular arrays of Au nanoparticles, which yields a remarkable resonance quality factor $Q \approx 40$ for the double-dot array measured from extinction and $Q \approx 60$ measured from the ellipsometry/reflection data for the single dots. By the resonance quality Q here we simply imply the ratio of the wavelength of the peak position over the peak width. This is almost an order of magnitude improvement compared with standard LPR in analogous gold nanodots [7]. It worth noting that the resonance quality in the ellipsometry/reflection for the double-dot array ($Q \approx 30$) was smaller than that calculated using the extinction data ($Q \approx 40$), which is explained by the properties of coupling of the diffracted mode with the localized plasmons.

Let us briefly discuss some other important experimental properties of the supernarrow resonances. We found that these resonances are observed mostly for the light of p polarization. When the Cr layer was removed, we observed narrow resonances for s polarization as well as for p polarization, although relative amplitudes of resonances changed more abruptly with AOI. (In addition, dipoles induced in the substrate affect both polarization differently [23].) The dipole nature of scattering required nonzero AOI to achieve coupling between incident light of p polarization and diffracted waves propagating along the surface of the samples. As a result, p resonances disappeared as AOI was decreased; see Figs. 3(a) and 3(b).

Figure 3(c) shows the dependence of the resonances half-width and the value of Ψ at the minimum as a function of the angle of incidence for the single dot array. It is worth stressing that the minimal half-width observed was just 5 nm. The reflected amplitude R_p goes close to zero twice at AOI = 48° and AOI = 64°. This implies that a regular array of metallic nanoparticle can have two different "Brewster conditions." For $a = 270$–500 nm in the spectral range of $\lambda = 240$ nm–1000 nm we have usually observed two air and two substrate resonances given by (1) with $m = 1$ and 2 and the sign "+", which corresponds to the diffraction mode propagating along the surface in the direction opposite to the tangential wave-vector of incident light; see Figs. 3(d)–3(f) where λ_R are superimposed onto the reflection spectra. The widths of resonances in reflection depend on the number of particles interacting with the diffracted mode and should decrease when the array con-

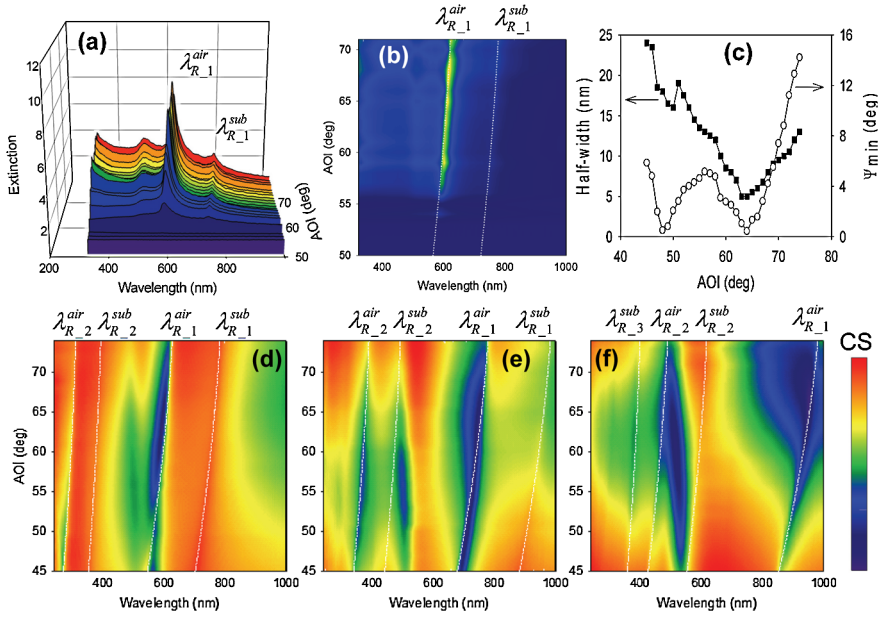

FIG. 3 (color online). Properties of supernarrow resonances. (a) The spectral dependence of extinction for the double-dot array of Fig. 2 plotted for AOIs = 50–74° for p polarization. (b) The 2D plot of the extinction shown in (a), image color scale CS from 0 to 12. (c) The angular dependence of the resonance half-width and the value of Ψ_{min} at the Wood anomaly for the single dot array of Fig. 1. The color maps of Ψ for the double-dot arrays with $d \approx 100$ nm, $h =$ 90 nm and (d) $a = 320$ nm, CS from 0° to 40°. (e) $a = 400$ nm, CS from 1° to 36°. (f) $a = 500$ nm, CS from 3° to 36°. The dotted white lines show $\lambda^{\text{air}}_{R\_m}$ and $\lambda^{\text{sub}}_{R\_m}$, which are given by (1) with the sign +.

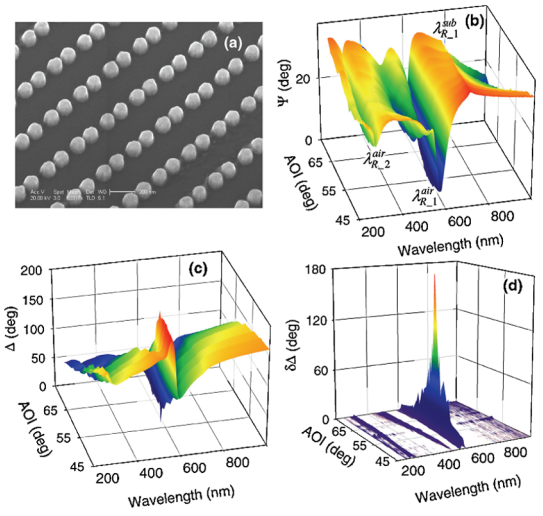

FIG. 4 (color online). Properties of the double-dot Au nanoarray with the period $a = 320$ nm, the dot diameter $d = 110$ nm, the dot height $h = 90$ nm. (a) The micrograph of the array obtained under a tilted angle. (b) 3D plot of Ψ-value as a function of AOI and wavelength, CS from 0° to 35°. $\lambda^{\text{air}}_{R\_m}$ and $\lambda^{\text{sub}}_{R\_m}$ are given by (1) with the sign + (c) 3D-plot of phase Δ, CS from 0° to 180°. (d) 3D plot of digital derivative of phase Δ.

stant a is increased at a fixed h. (The behavior of Schatz-Markel resonances in extinction is more complicated [12,13,24]). We did not observed such decrease in experiments. Figures 3(d)–3(f) shows that the resonance width in reflection slightly increased with a. There are three factors which contribute to this behavior: (a) glass curvature, (b) a finite size of the focal spot, and (c) a finite size of the spatial coherence of the beam. These factors decrease the effective number of dots interacting with diffracted waves and increase the resonance half-width for arrays with a larger period.

The best quality factor Q of supernarrow resonances has been achieved in arrays with the best quality and reproducibility of lithography. Figure 4(a) shows a micrograph of a double-pillar Au nanoarray taken under some angle demonstrating the degree of array uniformity. This sample has slightly larger diameter of double dots ($d = 110$ nm) and showed one "Brewster angle" at which *the reflection R_p was exactly zero* at some wavelength, see Figs. 4(b) and 4(c) that provide 3D graphs of Ψ and Δ dependence. Figure 4(c) shows a very sharp spike of the phase Δ at the position where $R_p = 0$. To explore this jump we plot the digital derivative of the phase $\delta\Delta(\lambda) = \Delta(\lambda + \delta\lambda) - \Delta(\lambda)$, with $\delta\lambda = 0.8$ nm in Fig. 4(d). Remarkably, the digital derivative equals 180° at the position where $R_p = 0$, which corresponds to Heaviside-like π-jump of the phase [25]. Such π-jumps of phase have been already discussed for the conventional surface plasmon resonance [25,26] and could be important for biosensing [27]. The observed resonances could be essential for a number of applications, e.g., nanotweezing [28], as well as for regular arrays of plasmonic devices including nanolenses, nanolasers, and field amplifiers. These resonances are spatially dispersive and have to be taken into account when describing optical properties of regular arrays of nanoparticles [29].

Authors thank Andre Geim, Bill Barnes and Roy Sambles for fruitful discussions. Work has been supported by Paul Instrument and EPSRC EP/E01111X/1 Grants.

[1] T. W. Ebbesen, Nature (London) **391**, 667 (1998).
[2] E. Altewischer, M. P. van Exter, and J. P. Woerdman, Nature (London) **418**, 304 (2002).
[3] C. Genet and T. W. Ebbesen, Nature (London) **445**, 39 (2007).
[4] J. B. Pendry, Phys. Rev. Lett. **85**, 3966 (2000).
[5] A. A. Houck, J. B. Brock, and I. L. Chuang, Phys. Rev. Lett. **90**, 137401 (2003).
[6] N. Fang, H. Lee, C. Sun, and X. Zhang, Science **308**, 534 (2005).
[7] A. N. Grigorenko *et al.*, Nature (London) **438**, 335 (2005).
[8] W. L. Barnes, A. Dereux, and T. W. Ebbesen, Nature (London) **424**, 824 (2003).
[9] S. A. Mayer *et al.*, Adv. Mater. **13**, 1501 (2001).
[10] F. Wang and Y. R. Shen, Phys. Rev. Lett. **97**, 206806 (2006).
[11] K. Li, M. I. Stockman, and D. J. Bergman, Phys. Rev. Lett. **91**, 227402 (2003).
[12] S. Zou, N. Janel, and G. C. Schatz, J. Chem. Phys. **120**, 10871 (2004).
[13] V. A. Markel, J. Phys. B **38**, L115 (2005).
[14] E. M. Hick *et al.*, Nano Lett. **5**, 1065 (2005).
[15] R. W. Wood, Philos. Mag. **4**, 396 (1902).
[16] Lord Rayleigh, Proc. R. Soc. A **79**, 399 (1907).
[17] R. M. A. Azzam and N. M. Bashara, "*Ellipsometry and Polarized Light*," (North-Holland, Amsterdam, 1977);
[18] M. Born and E. Wolf, *Principles of Optics* (Cambridge University Press, Cambridge, England, 1980).
[19] L. V. Panina, A. N. Grigorenko, and D. P. Makhnovskiy, Phys. Rev. B **66**, 155411 (2002).
[20] W. Rechberger *et al.*, Opt. Commun. **220**, 137 (2003).
[21] V. A. Podolskiy, A. K. Sarychev, E. E. Narimanov, and V. M. Shalaev, J. Opt. A Pure Appl. Opt. **7**, S32 (2005).
[22] A. N. Grigorenko, Opt. Lett. **31**, 2483 (2006).
[23] T. Yamaguchi, S. Yoshida, and A. Kinbara, Thin Solid Films **21**, 173 (1974).
[24] S. Zou and G. C. Schatz, J. Chem. Phys. **121**, 12 606 (2004).
[25] A. N. Grigorenko, P. I. Nikitin, and A. V. Kabashin, Appl. Phys. Lett. **75**, 3917 (1999).
[26] A. V. Kabashin and P. I. Nikitin, Opt. Commun. **150**, 5 (1998).
[27] P. I. Nikitin *et al.*, Sens. Actuators A, Phys. **85**, 189 (2000).
[28] A. N. Grigorenko, N. W. Roberts, M. R. Dickinson, and Y. Zhang, Nat. Photon. **2**, 365 (2008).
[29] F. J. Garcia de Abajo, Rev. Mod. Phys. **79**, 1267 (2007).